JOURNAL OF AIRCRAFT
Vol. 34, No. 3, May–June 1997

# Conceptual Fluid/Motion Coupling in the Herbst Supermaneuver

Lars E. Ericsson*
*Mt. View, California 94040*
and
Martin E. Beyers†
*Institute for Aerospace Research, Ottawa, Ontario K1A 0R6, Canada*

**A study of the unique problems introduced by the coupling between control demands and vehicle dynamics for advanced aircraft performing radical maneuvers shows that the fluid/motion coupling depends critically on the aircraft geometry and maneuver/time history. The goal of the exploratory analysis is to provide the vehicle designer with increased insight into the basic flow physics that can lead to troublesome coupling effects between control input and vehicle dynamics.**

## Nomenclature

$b$ = wing span
$c$ = wing mean aerodynamic chord
$d$ = maximum body diameter
$d(x)$ = local body diameter
$l$ = body length
$m$ = pitching moment, coefficient $C_m = m/q_\infty Sc$
$N$ = normal force, coefficient $C_N = N/q_\infty S$
$n$ = yawing moment, coefficient $C_n = n/q_\infty Sb$
$p$ = static pressure, coefficient $C_p = (p - p_\infty)/q_\infty$
$q_\infty$ = dynamic pressure, $\rho_\infty U_\infty^2/2$
$Re$ = Reynolds number, $U_\infty d/\nu_\infty$, $Re(x) = U_\infty d(x)/\nu_\infty$
$r$ = yaw rate
$S$ = reference area, $\pi d^2/4$ for body alone; projected wing area for aircraft
$t$ = time
$U_\infty$ = freestream velocity
$V$ = resultant crossflow velocity
$x$ = axial distance from apex
$Y$ = side force, coefficient $C_Y = Y/q_\infty S$
$\alpha$ = angle of attack
$\beta$ = angle of sideslip
$\theta_A$ = apex half angle
$\nu$ = kinematic viscosity
$\rho$ = air density
$\sigma$ = body axis inclination relative to the velocity vector
$\phi$ = body azimuth
$\psi$ = coning angle
$\Omega$ = dimensionless coning rate, $\dot{\psi}b/2U_\infty$

*Subscripts*
$A$ = apex
$a$ = attached flow
CG = center of gravity or rotation center
cr = critical
$m$ = motion induced
$N$ = nose
$V$ = vortex
2D = two dimensional
$\infty$ = freestream condition

*Derivative Symbols*
$C_{nr}$ = $\partial C_n/\partial(br/2U_\infty)$
$C_{n\dot{\beta}}$ = $\partial C_n/\partial(b\dot{\beta}/2U_\infty)$
$\dot{\psi}$ = $\partial\psi/\partial t$

## Introduction

AERODYNAMIC coupling between vehicle motion and dynamically separated flows can generate moments that strongly interact with control-commanded moments. This has important implications for high-alpha flight control. The classic supermaneuver concept introduced by Herbst[1] (Fig. 1) is an appropriate model for this discussion. Quoting Herbst[1]: ''One of the most applicable analytic maneuvers, for example, is that of a 180° change of heading with the additional constraint of returning to the point of departure at initial speed and altitude.'' This maneuver involves a coning motion, otherwise known as a velocity vector roll, and is kinematically similar to a yawing motion at high alpha. No significant body-axis rolling motion is involved in the heading change, but sig-

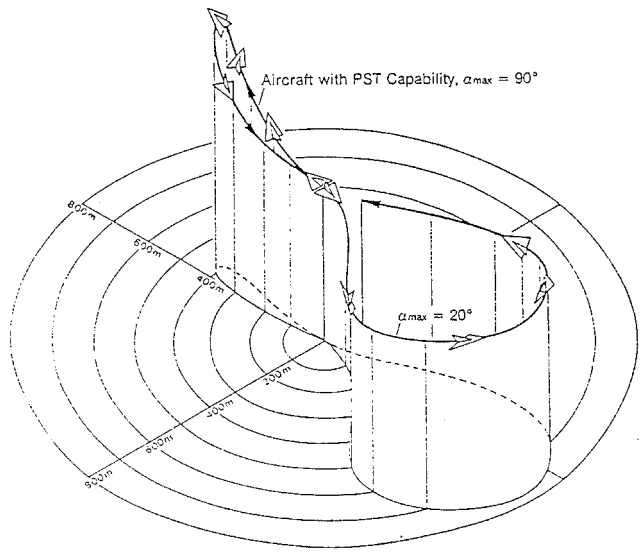


**Fig. 1 Herbst supermaneuver.[1]**

Presented as Paper 96-0787 at the AIAA 34th Aerospace Sciences Meeting, Reno, NV, Jan. 15–19, 1996; received June 17, 1996; revision received Dec. 22, 1996; accepted for publication Dec. 23, 1996. 

*Engineering Consultant. Fellow AIAA.
†Head Aircraft Aerodynamics Group, Aerodynamics Laboratory. Senior Member AIAA.

nificant Mach number excursions occur during the pitch-up. The unsteady aerodynamics producing the fluid/motion coupling are distinctly different for two categories of advanced aircraft geometries. For slender-wing aircraft the high-alpha aerodynamics are dominated by the loads induced by wing leading-edge vortices, whereas for the slender-nosed aircraft large asymmetric loads are generated by the forebody. Only the latter aircraft category will be considered in the present paper.

## Analysis

When the aircraft has a slender nose ($l_N/d > 2$), as in the case of the X-31 aircraft[2] shown in Fig. 2, the coupling between control demands and vehicle dynamics becomes very different from that for a slender-wing aircraft. The flow separation of concern occurs on the slender nose rather than at the wing leading edges. When wing and leading-edge extension (LEX) surfaces are located far behind the slender nose, as in the case of the F-14 Tomcat[3] (Fig. 3), the forebody crossflow separation depends strongly on the vehicle motion through so-called moving wall effects.[4] When the wing and/or LEX surfaces start at the base of the slender forebody, as exemplified by the F-16 Fighting Falcon[5] (Fig. 4), it is found that the wing-induced upwash tends to overpower the moving wall effect. Both types of aircraft geometry will be analyzed.

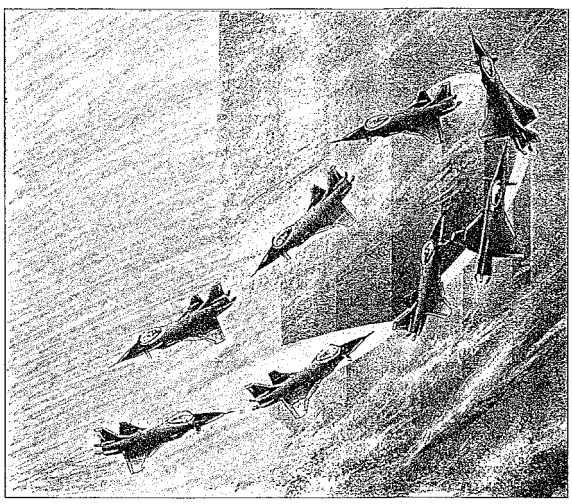

**Fig. 2 X-31 performing the Herbst maneuver.[2]**

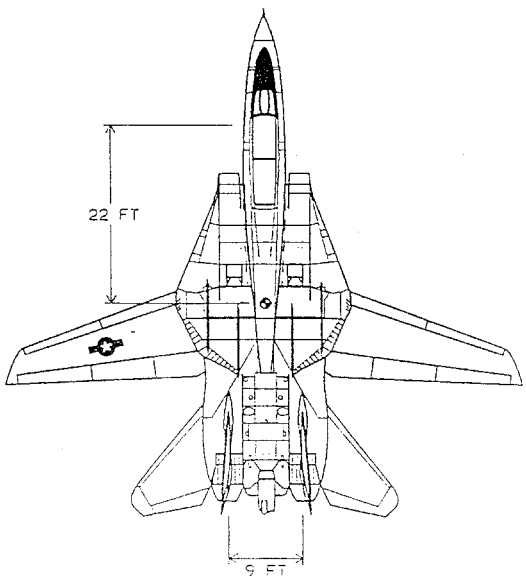


**Fig. 3 F-14 Tomcat.[3]**

### Wing and LEX Well Downstream of a Slender Forebody

Tests of a wind-tunnel model with this type of aircraft geometry[6] have demonstrated that the huge, rate-induced yawing moments measured at high angles of attack are largely generated by the loads on the slender forebody (Fig. 5), and body-alone lateral–directional aerodynamic results are in this case representative of the complete aircraft.

It is well known that nose microasymmetries affect the high-alpha crossflow separation on a slender, axisymmetric body.[7] In view of this fact, the experimental results for a cone–cylinder body, free to roll around the velocity vector[8,9] (Fig. 6), are of considerable interest. The test results demonstrate that

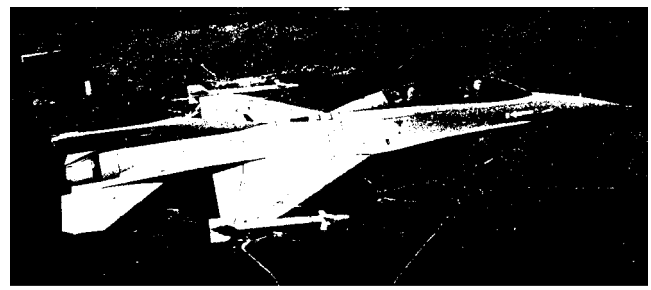

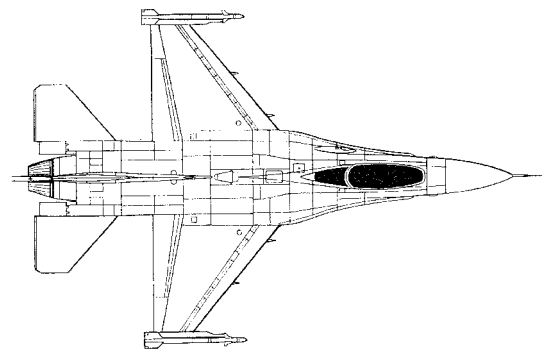

**Fig. 4 F-16 Fighting Falcon.[5]**

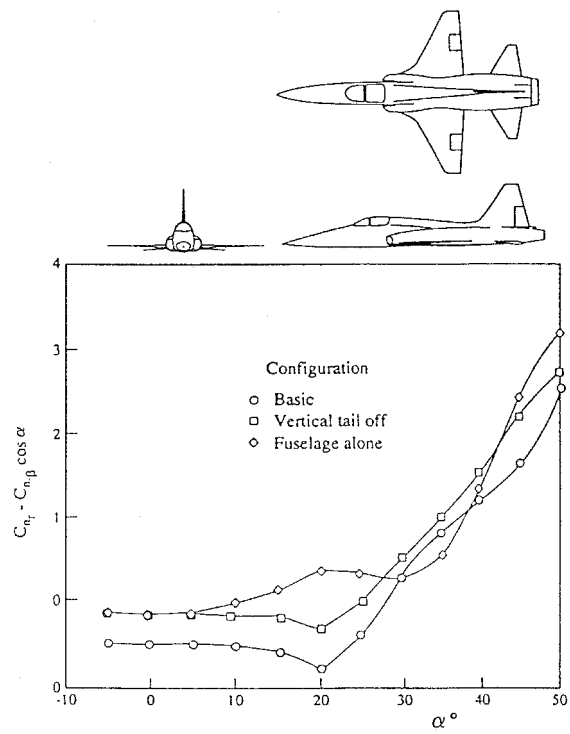


**Fig. 5 Yaw damping characteristics of an advanced aircraft model.[6]**

during the initial spin-up of the coning motion the effect of roll-angle, which is large in static tests at similar, laminar test conditions,[7] is completely overpowered by the moving wall effect.[4] At full-scale Reynolds numbers the largest region of crossflow separation occurs for supercritical flow conditions, with a similar type of proconing coupling between crossflow separation and vehicle motion as in the subcritical case[4] (Fig. 6).

On a maneuvering aircraft of the type under discussion it is the moving wall effect acting in the boundary layer buildup region, near the crossflow stagnation line on the nose, that determines the flow separation asymmetry. Furthermore, as the coning associated with the supermaneuver will occur at high angles of attack, 45 deg < α < 90 deg, flat-spin results for axisymmetric bodies[10] provide useful information. The static experimental results for a 5.4-deg cone–cylinder[11] (Fig. 7) show that the local crossflow Reynolds number $Re(x)$ is a good indicator of the type of symmetric or asymmetric separation that will occur. Figure 7 shows that the first side-force peak, point C, is caused by subcritical/critical crossflow separation. In the static case the force can be positive or negative. However, in flat-spin the crossflow separation establishes itself in a direction that produces an antispin moment[4] (Fig. 8). At points D and E in Fig. 7, the two-bubble, symmetric, critical/critical separation geometry is established. When perturbed by a translatory motion of the cross section, this separation type also produces an antispin moment, as demonstrated by Polhamus' experimental results[10,12] in Fig. 9 for Ω < 0.25. Finally, when the Reynolds number has been increased to point F in Fig. 7, the pro-spin supercritical/critical crossflow separation is established (see inset for Ω > 0.5 in Fig. 9).

While the flat spin characteristics of advanced aircraft are very similar to those of axisymmetric bodies, the mechanisms initiating the flat spin are quite different. The flat spin of the axisymmetric body is initiated by a static moment generated at α = 90 deg through the effects of asymmetrically distributed body-roughness.[10] The large static moment is able to accelerate

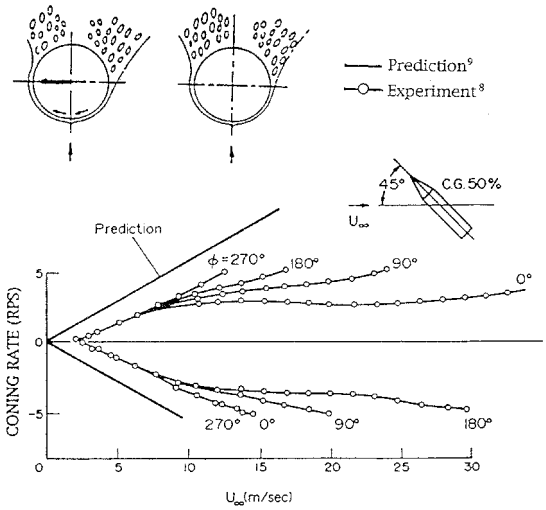


**Fig. 6 Free-to-spin coning rate of cone–cylinder.[8,9]**

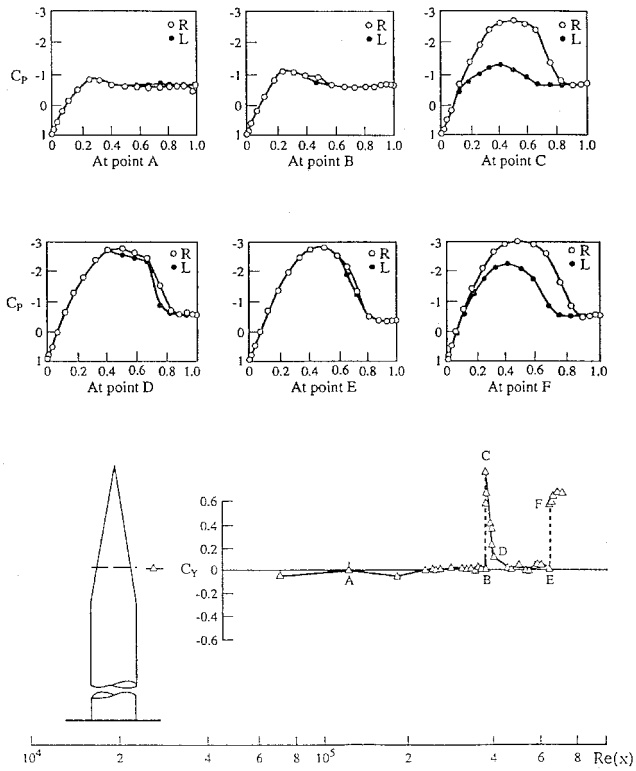


**Fig. 7 Cross-sectional pressure distributions on a 5.4-deg cone–cylinder at α = 90 deg.[11] R and L refer to the right and left halves, respectively, of the cone–cylinder at α = 90 deg. The abscissa is the vertical cross-sectional distance between surface points and the flow stagnation point. Thus, the enclosed area between the curves labeled R and L represents the local side force.**

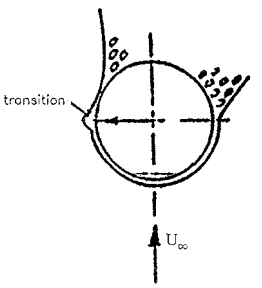


**Fig. 8 Subcritical/critical separation on a circular cross section moving to the right.**

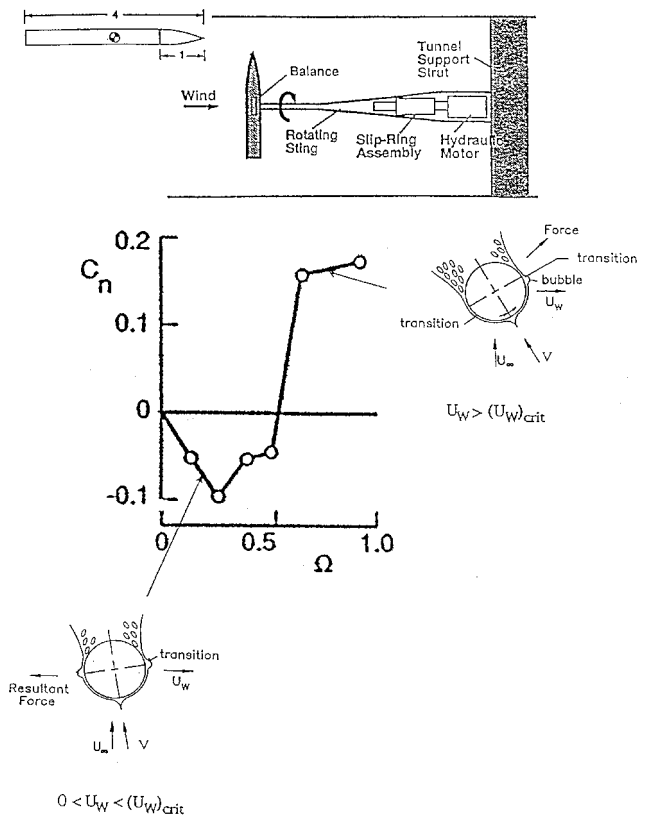


**Fig. 9 Flat-spin yawing moment at critical flow conditions in Polhamus' flat-spin test.[12]**

the flat spin through the spin-resisting subcritical/critical (Fig. 8) and critical/critical (Fig. 9 for $\Omega < 0.5$) regions of crossflow separation to the final pro-spin supercritical/critical separation, shown in Fig. 9 for $\Omega > 0.5$. This results in the experimentally observed flat-spin characteristics[13] shown in Fig. 10. Figure 10 shows that asymmetric crossflow separation is subject to the usual hysteresis effects. In the case of the Herbst supermaneuver,[1] the initiation of the translatory motion of the circular cross section is driven by the control-induced moment. As a rapid roll around the velocity vector is demanded, the supercritical/critical flow separation (Fig. 9 for $\Omega > 0.5$) is established directly over a significant portion of the critical flow region on the slender forebody, adding to the pro-coning contribution from the downstream supercritical/supercritical crossflow separation on the slender forebody. This action would occur in the entire range, 45 deg $< \alpha <$ 90 deg. Thus, the moving wall effect will significantly amplify the control-induced yawing moment. In addition, a sudden increase of the pitch-up moment will be generated by the change to an asymmetric crossflow separation geometry. The experimental results for a five-caliber tangent–ogive[14] (Fig. 11) show that the separation asymmetry in addition to generating a side force $C_Y$ also produces an increase of the normal force $C_N$. Experimental results for the effect of a nose strake on a pointed ogive–cylinder[15] (Fig. 12) indicate that the normal force can be increased substantially at $\alpha > 35$ deg through the change from symmetric to asymmetric crossflow separation. Recent tests[16] showed that removing the nose strakes on an advanced aircraft model, thereby allowing the development of static, asymmetric crossflow separation, more than doubled the nose-up pitching moment (Fig. 13). Thus, a strong pitch-up tendency is associated with the crossflow separation asymmetry established during a rapid roll around the velocity vector. This could have provided the conditions for a stable, steep spin mode of the F-14 aircraft at $\alpha > 50$ deg.[17]

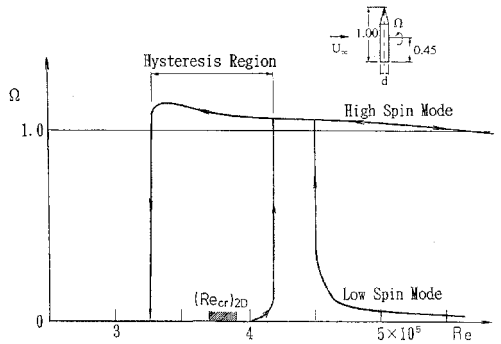


**Fig. 10 Flat-spin characteristics of cone–cylinder.[13]**

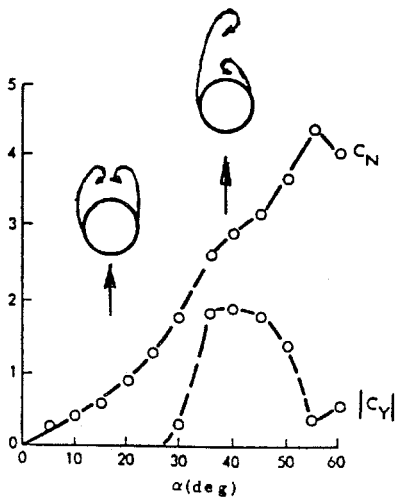


**Fig. 11 Effect of crossflow separation asymmetry on $C_Y$ and $C_N$ of a five-caliber tangent–ogive.[14]**

### Wing and/or LEX Located Close to a Slender Forebody

The wing rock observed in tests with a generic aircraft model[18] (Fig. 14) was caused by moving wall effects generated by a rolling motion rather than coning.[19] Moving the wing forward to the base of the slender nose eliminated the wing rock that occurred with the wing in the aft position. It was suggested in Ref. 20 that the explanation was that in the forward position the wing-induced upwash overpowered the moving wall effects, thereby eliminating the flow mechanism driving the wing rock. The shaded LEX surfaces, added in the

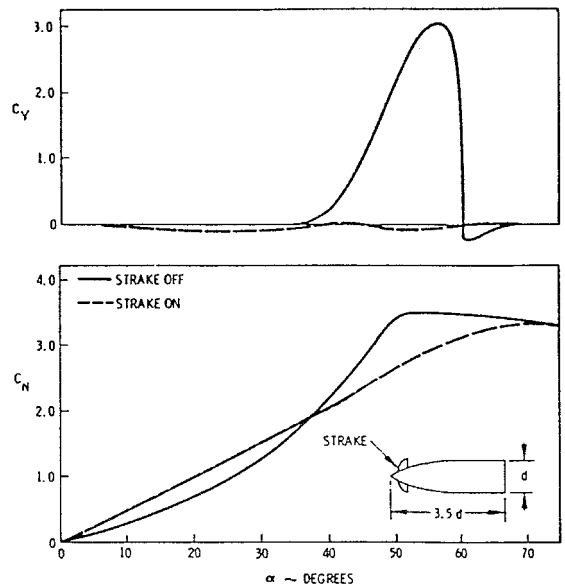


**Fig. 12 Effect of nose strake at $Re = 0.35 \times 10^6$ on $C_Y$ and $C_N$ of ogive–cylinder body.[15]**

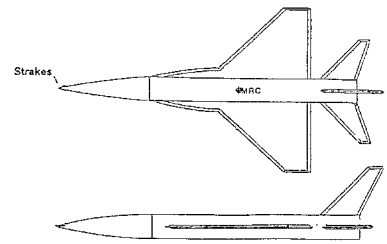


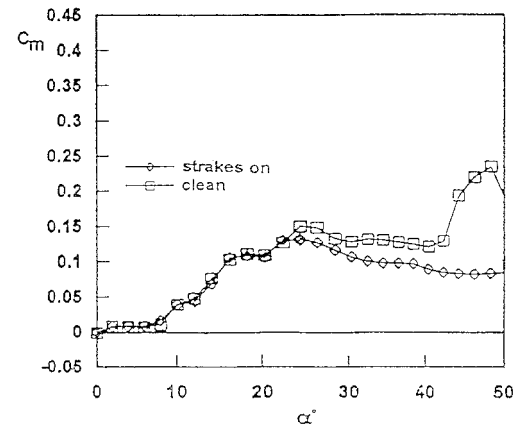


**Fig. 13 Effect of nose strakes on $C_m(\alpha)$ of a generic AGARD aircraft model.[16]**

right-hand sketch of Fig. 14, could probably have accomplished the same thing. Recent experimental results[21] indicate that this would indeed have been the case. The LEX geometry shown in Fig. 13, similar to that illustrated in Fig. 14, delayed the occurrence of static, asymmetric crossflow separation on the slender forebody to above the expected value[7] $\alpha = 2\theta_A = 28.5$ deg.

Figure 15 illustrates the effect of the LEX-induced upwash on the forebody in the case of a coning motion. The coning rate generates a sideslip that decreases the effective leading-edge sweep of the LEX surfaces on the advancing side and increases it on the receding side. The result is a stronger LEX-induced upwash on the advancing side than on the receding side, as indicated in Fig. 15b. This situation prevails until vortex breakdown has moved to the LEX apex, causing a loss of the upwash generated by the spiral vortex downstream of vortex breakdown. As a consequence of the dominance of the LEX-induced upwash over the moving wall effects, discussed earlier, the crossflow separation and associated vortex shedding on the slender forebody is changed. Instead of generating a pro-spin force as in the case of no LEX surfaces (Fig. 15a), the LEX-induced upwash causes the crossflow separation to generate an antispin force on the forebody (Fig. 15b). Figure 16 shows flow visualization results at $\alpha = 32$ deg and a small angle of sideslip for a model of a slender-nosed aircraft with LEX surfaces, the F-18L aircraft.[22] It can be seen that the LEX-induced upwash generated the vortex asymmetry sketched in Fig. 15b.

Because of the large effect of the asymmetric forebody flow separation on the dynamics of an advanced aircraft, it became obvious that some form of control of the forebody crossflow separation was needed. The initial effort was to try to eliminate or greatly reduce the flow asymmetry.[7] Presently, however, the more ambitious goal is to be able to control the asymmetry,[23,24] thereby achieving the desired supermaneuverability.[1] The main effort has so far been almost exclusively focused on the achievable control capability, whereas the mutual interaction between control application and vehicle unsteady aerodynamics has received very little attention. One problem is to account for the large effect of roll angle on the control effectiveness of fixed controls, such as forebody strakes, as illustrated by the experimental results[25] in Fig. 17. On the maneuvering aircraft the crossflow stagnation point will continually change its position relative to the control surfaces. In the case of the dual, rotatable tip-strakes in Fig. 17, a 10-deg rotation of the crossflow stagnation point would at $\alpha = 55$ deg change the yawing moment coefficient $C_n$ from approximately 0.06 at $\phi = 0$ to $-0.06$ at $\phi = 10$ deg. For an aircraft in a coning motion, the rotation of the crossflow stagnation point at station $x$ caused by the coning-induced lateral velocity is

$$\phi_m = \tan^{-1}[2(x_{CG}/b - x/b)(\Omega b/2U_\infty)] \qquad (1)$$

For $\Omega b/2U_\infty = 0.15$, Eq. (1) gives $\phi_m > 10$ deg over most of the slender nose of a typical fighter configuration. Placing the strakes or blowing ports on the top side avoids this problem of the changing flow stagnation point, and can still provide satisfactory control, as has been demonstrated for the F-18 HARV.[26] However, forebody blowing will decrease in effectiveness as the angle of attack is increased into the $\alpha$ range for steady asymmetric crossflow separation.

The difficulty in performing the Herbst supermaneuver with a slender-nosed aircraft was overcome by using thrust vectoring on the X-31 aircraft (Fig. 2). Test pilot Karl Lang performed the supermaneuver, using a turning radius of 475 ft compared to the 2700-ft radius of a coordinated, steady turn.[2] To decouple lateral and longitudinal control mechanisms, as was accomplished here by using thrust vectoring for lateral control and all movable canards for pitch control, appears to be important to minimize the tendency toward adverse control/

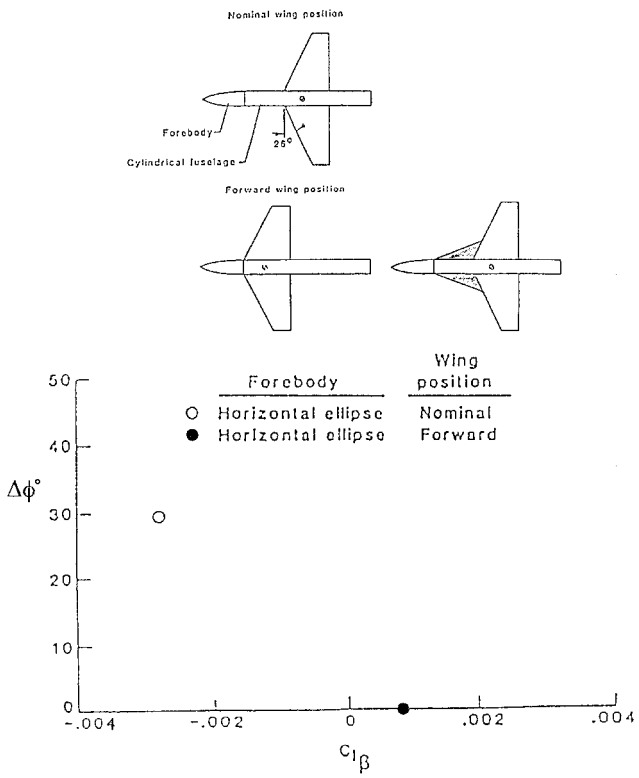


**Fig. 14 Forebody-induced wing rock of generic aircraft model at $\alpha = 30$ deg.[18]**

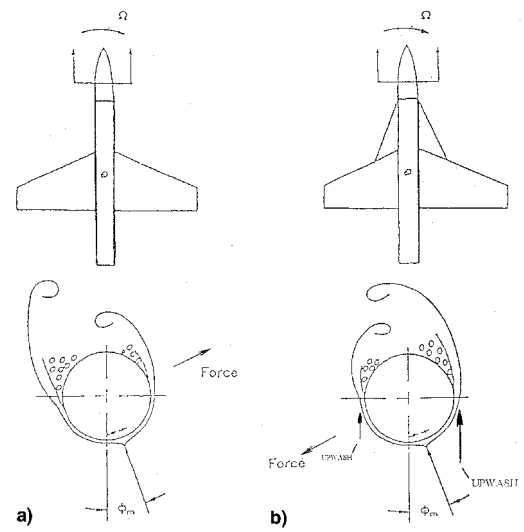


**Fig. 15 Crossflow separation on coning slender forebody: a) without and b) with LEX.**

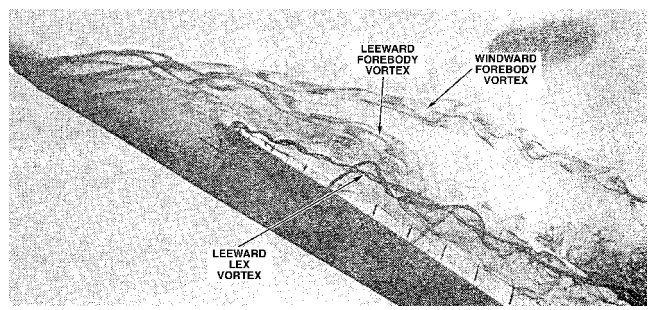


**Fig. 16 Effect of sideslip at $\alpha = 32$ deg on forebody vortices of the F-18L in the presence of LEX surfaces.[22]**

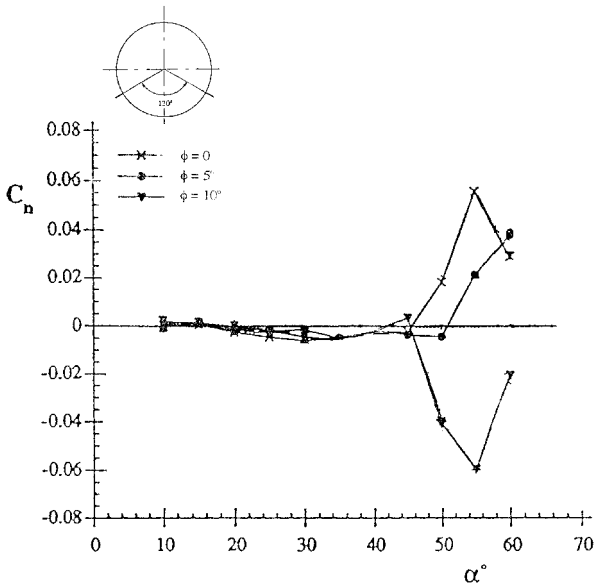


**Fig. 17 Effect of rotatable dual-tip strakes on the yawing moment of an F/A-18 model.[23]**

vehicle dynamics coupling.[27] Moreover, for symmetric deflection, the induced upwash by canards with swept leading edges will generate an antispin force on the forebody in the presence of a coning motion (see the earlier discussion of Fig. 15).

## Maneuver Time History

The question that has to be answered to assess the lateral–directional control requirements in the supermaneuver is whether or not asymmetric flow separation conditions will be established over some part of the alpha range. Considerations of the flight conditions should in themselves give an indication of the likelihood of departure.

The entry into the poststall maneuver (Fig. 1) occurs at high subsonic Mach numbers, where the crossflow separations are predominantly of the supercritical type. At moderate altitudes the flow conditions are likely to remain supercritical during the deceleration period when the angle of attack climbs into the range for asymmetric crossflow separation. Since the coning motion is initiated before that point, there is a possibility of departure into a steep spin when the pitching moment changes sign at high alpha. With further deceleration as alpha approaches 90 deg, the critical/supercritical crossflow separation is established over part of the forebody, facilitating the departure into flat spin. Thus, for forebody-dominated aircraft configurations the danger of departure would be present at more than one segment of the Herbst maneuver.[1] Consequently, even if the aircraft manages to traverse the $\alpha$ range for asymmetric crossflow separation uneventfully, the control-induced lateral motion can lead to flat spin when the critical/supercritical flow asymmetry occurs at 70 deg $< \alpha <$ 90 deg. The commanded maximum yaw rate of the F-14 aircraft,[3] 180 deg/s, would result in a lateral velocity of roughly 100 fps at the nose tip (Fig. 3). For $M_\infty < 0.2$ this would result in $\Omega >$ 0.5, generating a flat-spin-driving moment according to Fig. 9.

Even in the absence of a control-induced input, the forebody flow is likely to be asymmetric from $\alpha > 2\theta_A$ up to angles of attack approaching 90 deg, because of the flowfield time lag. For initially supercritical flow conditions the supercritical/critical separation asymmetry (point F in Fig. 7) could be established as $\alpha$ approaches 90 deg. Thus, departure into flat spin is possible. This tendency will be independent of the presence of nose strakes, because at these high incidences asymmetric crossflow separation will develop on the forebody aft of the strakes.[28] This behavior has been observed for the X-31 at $\alpha \geq$ 60 deg (Ref. 29) as well as for the AGARD WG16 model[21] at $\alpha \geq$ 45 deg. Also, maneuver control through forebody blowing[23] will be ineffective at very high angles of attack.

In contrast to the Herbst supermaneuver,[1] where a large control-induced yaw rate will be generated and favoring departure into flat spin in the case of a pitch-up to $\alpha$ = 70 deg, the steep spin that might result at the equilibrium conditions will occur at a lower rotation rate and possibly higher angle of attack because of the reduced pitch-down moment in the presence of asymmetric crossflow separation. On the other hand, if the aircraft is pitched up toward $\alpha$ = 90 deg, the full negative pitching moment generated by the tail surfaces has to be balanced, leading to a fast flat spin that is generally not recoverable. The conditions for spin equilibrium also require a balance of lateral forces, which is provided at finite sideslip. In the analysis of incipient departure it is also necessary to consider inertial cross-coupling,[30] a task beyond the scope of the present paper, the purpose of which is to draw attention to the unsteady aerodynamic effects that have to be included for realistic high-alpha flight dynamics prediction.

The conditions associated with fluid/motion coupling at lower altitudes are dangerous to cover in flight tests and difficult to investigate in wind tunnels because of the high Reynolds numbers that have to be simulated. As a result, very little data is available for these flow conditions. Consequently, more analysis is needed of fluid/motion coupling at high subsonic Mach numbers and high Reynolds numbers.

## Conclusions

An analysis of the Herbst supermaneuver shows that one principal source of the highly nonlinear fluid/motion coupling effects at high angles of attack is the effect of the vehicle motion on the asymmetric crossflow separation on a slender forebody. The potential for adverse control/motion coupling is a strong function of aircraft geometry, altitude, and maneuver characteristics. The presence of LEX surfaces are found to have a profound effect on the maneuver characteristics of a slender-nosed aircraft. Forebody-dominated aircraft experience a larger alpha range of departure-prone behavior than their LEX-dominated counterparts. The nature of, and response to, the fluid/motion coupling effects are governed by the maneuver time history.

## References

[1]Herbst, W. B., "Supermaneuverability," *Proceedings of Workshop on Unsteady Separated Flow*, edited by Francis and Luttges, U.S. Air Force Academy, 1983, pp. 1–9.

[2]Brown, S. F., "It Went Thataway," *Popular Science*, Oct. 1993, p. 26.

[3]Goodman, R. J., and Conigliaro, P. E., "F-14A Low Altitude High Angle of Attack Simulation and Flight Test Program," AIAA Paper 86-9774, April 1986.

[4]Ericsson, L. E., "Moving Wall Effects in Unsteady Flow," *Journal of Aircraft*, Vol. 25, No. 11, 1988, pp. 977–990.

[5]*Jane's All the World's Aircraft*, edited by John W. R. Taylor, Jane's Information Group, Ltd., Coulsdon, Surrey, UK, 1989, p. 412.

[6]Grafton, S. B., Chambers, J. R., and Coe, P. L., Jr., "Wind-Tunnel Free-Flight Investigation of a Model of a Spin Resistant Fighter Configuration," NASA TN D-7716, June 1974.

[7]Ericsson, L. E., and Reding, J. P., "Asymmetric Flow Separation and Vortex Shedding on Bodies of Revolution," *Tactical Missile Aerodynamics: General Topics*, edited by M. J. Hemsch, Vol. 141, Progress in Astronautics and Aeronautics, AIAA, Washington, DC, 1992, pp. 391–452, Chap. 10.

[8]Yoshinaga, T., Tate, A., and Inoue, K., "Coning Motion of Slender Bodies at High Angles of Attack in Low Speed Flow," AIAA Paper 81-1899, Aug. 1981.

[9]Ericsson, L. E., "Prediction of Slender Body Coning Characteristics," *Journal of Spacecraft and Rockets*, Vol. 28, No. 1, 1991, pp. 43–49.

[10]Ericsson, L. E., and Beyers, M. E., "On the Flat Spin of Axisymmetric Bodies," *Journal of Aircraft*, Vol. 32, No. 6, 1993, pp. 1205–1212.

[11]Kamiya, N., Suzuki, S., Nakamura, M., and Yoshinaga, T., "Some Practical Aspects of the Burst of Laminar Separation Bubbles," International Council of the Aeronautical Sciences, 80-10.2, Sept. 1980.

[12]Ericsson, L. E., and Beyers, M. E., "Viscous-Flow/Vehicle-Motion Coupling," *Fluid Dynamics of Rotary Flows, Rotary Balance Testing for Aircraft Dynamics*, AGARD-AR-265, Dec. 1990, pp. 164–167, 183–187, Chap. 8.

[13]Tate, A., Iwasaki, A., Fujita, T., and Yoshinaga, T., "Flat Spin of Axisymmetric Bodies near the Critical Reynolds Number Region," National Aerospace Lab., TR-1271, June 1995 (in Japanese).

[14]Keener, E. R., Chapman, G. T., Cohen, L., and Taleghani, J., "Side Forces on Forebodies at High Angles of Attack and Mach Numbers from 0.1 to 0.7. Two Tangent Ogives and Cone," NASA TMX-3438, Feb. 1977.

[15]Coe, P. L., Jr., Chambers, J. R., and Letko, W., "Asymmetric Lateral-Directional Characteristics of Pointed Bodies of Revolution at High Angles of Attack," NASA TN D-7095, Nov. 1972.

[16]Anon., "Cooperative Programme on Dynamic Wind Tunnel Experiments for Manoeuvering Aircraft," AGARD FDP WG16, AGARD-AR-305, Oct. 1996, Chap. 5.

[17]Jahnke, C. C., and Culick, F. E. C., "Application of Bifurcation Theory to the High-Angle-of-Attack Dynamics of the F-14," *Journal of Aircraft*, Vol. 31, No. 1, 1994, pp. 26–34.

[18]Brandon, J. M., and Nguyen, L. T., "Experimental Study of Effects of Forebody Geometry on High Angle of Attack Stability," *Journal of Aircraft*, Vol. 25, No. 7, 1988, pp. 591–597.

[19]Ericsson, L. E., "Wing Rock Generated by Forebody Vortices," *Journal of Aircraft*, Vol. 26, No. 2, 1989, pp. 110–116.

[20]Ericsson, L. E., "Further Analysis of Wing Rock Generated by Forebody Vortices," *Journal of Aircraft*, Vol. 26, No. 12, 1989, pp. 1098–1104.

[21]Cai, H. J., and Beyers, M. E., "Oscillatory Experiments on the AGARD WG16 Model," National Research Council, Inst. for Aerospace Research, AN-83, Ottawa, ON, Canada, Sept. 1995.

[22]Skow, A. M., and Erickson, G. E., "Modern Fighter Aircraft Designs for High Angles of Attack," AGARD-LS-121, Dec. 1982, pp. 4.1–4.59 (Paper 4).

[23]Malcolm, G. N., "Forebody Vortex Control," *Progress in Aerospace Sciences*, Vol. 28, 1991, pp. 171–234.

[24]Ericsson, L. E., "Control of Forebody Flow Asymmetry, a Critical Review," AIAA Paper 90-2833, Aug. 1990.

[25]Suarez, C. J., and Malcolm, G. N., "Water Tunnel Force and Moment Measurements on an F/A-18," AIAA Paper 94-1802, June 1994.

[26]Murri, D. G., Shah, G. H., DiCarlo, D. J., and Trilling, T. W., "Actuated Forebody Strake Controls for the F-18 High Alpha Research Vehicle," AIAA Paper 93-3675, Aug. 1993.

[27]Huber, P., and Galleithner, H., *X-31A High Angle of Attack and Initial Post Stall Flight Testing*, CP-519, AGARD, May 1992 (Paper 11).

[28]Beyers, M. E., and Ericsson, L. E., "Extraction of Subscale Free-Flight Aerodynamics from Rotary Tests of Combat Aircraft," AIAA Paper 97-0730, Jan. 1997.

[29]Alcorn, C. W., Croom, M. A., and Francis, M. S., "The X-31 Experience: Aerodynamic Impediments to Post-Stall Agility," AIAA Paper 95-0362, Jan. 1995.

[30]Kalviste, J., "Coupled Static and Dynamic Stability Parameters," AIAA Paper 89-3336, Aug. 1989.